JOURNAL OF CATALYSIS 29, 451–462 (1973)

Viscous and Diffusive Transport with Simultaneous Chemical Reaction in Non-Isobaric Porous Catalyst Particles

M. A. APECETCHE, M. G. GONZALEZ, R. J. J. WILLIAMS,[1] AND R. E. CUNNINGHAM[2]

Departamento de Tecnología Química, Fac. de. Ciencias Exactas, Universidad Nacional de La Plata, La Plata, Argentina

Received October 20, 1972

The effect of the pressure gradient produced by a nonequimolar chemical reaction upon the effectiveness factor in a spherical catalyst pellet is analyzed. A binary gaseous mixture under isothermal conditions is studied taking into account mass transfer due to the following mechanisms: viscous flow, nonequimolar flow, bulk diffusion and Knudsen diffusion. An irreversible, *m*th order reaction kinetics with respect to the gaseous reactant is assumed. Equations governing mass transfer with chemical reaction in the porous medium are developed on the basis of the dusty gas model. By numerical solution of these equations it is shown the nonisobaric effectiveness factor is considerably different from the isobaric one for every flow and diffusion regime. Besides, the Kramers-Kistemaker effect is observed when plotting the maximum pressure difference in the catalyst pellet as a function of the external pressure.

NONENCLATURE

A,B	reaction components
c_0	permeability of the porous medium, L^2
D_{AB}	bulk effective diffusivity, L^2/T
D_{AB}^0	coefficient independent of pressure, $D_{AB}^0 = D_{AB}\,P$, $M\ 1/T^3$
D^K	Knudsen effective diffusivity, L^2/T
D^*	dimensionless parameter defined below Eq. (31)
D^R	resultant effective diffusivity, $1/D^R = (P_0/D_{AB}^0) + (1/D_{AA}^K)$, L^2/T
h_0	generalized Thiele modulus defined below Eq. (31)
H^*	dimensionless parameter defined below Eq. (31)
k	specific constant of chemical reaction rate
M	molecular weight, M/mol
m	reaction order
N	molar flux, mol/L^2T
n	stoichiometric coefficient of the chemical reaction
P^*	dimensionless pressure, $P^* = P/P_0$
P	pressure, M/LT^2
R_0	radius of the catalyst pellet, L
R	gas constant, ML^2/T^2 mol θ
r_A	chemical reaction rate, mol/L^3T
r	radial position in the catalyst pellet, L
r^*	dimensionless radial position, $r^* = r/R_0$
T	absolute temperature, θ
y	mole fraction
y^*	dimensionless mole fraction, $y^* = y/y_0$
η	effectiveness factor
Φ	coefficient defined by Eqs. (16) and (17)
μ	viscosity, M/LT

---

[1] Research fellow of the Consejo Nacional de Investigaciones Científicas y Técnicas, Buenos Aires, Argentina.

[2] Member of Carrera del Investigador Científico of the Consejo Nacional de Investigaciones Científicas y Técnicas, Buenos Aires, Argentina. Also at: Laboratorio de Ensayo de Materiales e Investigaciones Tecnológicas (LEMIT), La Plata, Argentina.

Subscripts

0	evaluated at the boundary of the catalyst pellet
1	indicates a diffusive flux
2	indicates a viscous flux
m	indicates gaseous mixture

INTRODUCTION

Let us consider the following gas-phase reaction taking place in a porous catalytic pellet,

$$A_{(g)} = nB_{(g)}. \qquad (1)$$

When the reaction given by Eq. (1) takes place, composition gradients are developed inside the pellet and, if $n \neq 1$, pressure gradients will also arise in the system. Hence, mass can be transfered by four mechanisms viscous and nonequimolar flow, and Knudsen and bulk diffusion.

The influence of the volume change upon the effectiveness factor of the reaction has been studied (*1*, *2*), considering an isothermal isobaric system and bulk diffusion regime.

In order to study the effect of pressure gradients upon mass transfer in the porous medium, appropriate equations must be obtained. R. B. Evans III, G. M. Watson, and E. A. Mason developed the dusty gas model (*3–5*), which considers the porous medium as an array of dusty particles held fixed in space. Gas-surface interactions are taken into account by assuming dust particles are giant molecules, thus capable of being described by the equations of the kinetic theory of gases. From this viewpoint, equations governing the effects of pressure, temperature and composition gradients upon mass transfer in the porous medium are derived.

Assuming the validity of the dusty gas model equations, S. Otani, N. Wakao and J. M. Smith (*6*, *7*) studied the nonisobaric effectiveness factor of porous media. By analyzing the reaction given by Eq. (1), and considering isothermal steady state conditions and a first order irreversible reaction, the following results were obtained:

(a) The nonisobaric and isobaric effectiveness factors are identical for Knudsen diffusion regime.

(b) For bulk diffusion or Poiseuille flow regime the nonisobaric effectiveness factor is lower than the isobaric one for $n > 1$, and is higher for $n < 1$, in agreement with the positive direction of the pressure gradient which is developed in each case. However, it is shown the deviations between both effectiveness factors are lower than 10% in most actual conditions.

(c) The pressure gradients in the catalyst pellet reaches its maximum value when mass transfer is produced by Knudsen diffusion.

In a more recent study (*8*), E. A. Mason, A. P. Malinauskas, and R. B. Evans III consolidate and extend the kinetic theory foundations of the dusty gas model. The total flux of one of the components of a binary gaseous mixture under pressure gradients is obtained by adding the diffusive and viscous fluxes

$$N_A = N_{A1} + y_A(N_A + N_B)_2, \qquad (2)$$

where N_A is the total flux of the component A, and the subscripts 1 and 2 indicate diffusive and viscous fluxes, respectively. Here, the authors point out a mistake in their previous developments (*3–5*), where N_{A1} was considered as the total flux of the component A, even under pressure gradients, provided the effects of pressure on the bulk diffusion coefficient had been taken into account.

As previous papers (*6–7*) dealing with nonisobaric effectiveness factors assumed in their developments the validity of the incorrect equations developed in the original dusty gas model, it is obvious the necessity of rebuilding the whole problem.

Finally, R. D. Gunn and C. Judson King (*9*) developed an equation for mass transfer in porous media with pressure and composition gradients, based on the dusty gas model extended theory (*8*). However, these authors did not consider the effect of a chemical reaction. The theoretical results, which may be reduced to every particular case, were experimentally checked in nonisobaric porous media.

The aim of the present paper is two-fold:

(1) Determination of the effect of the different parameters of the system on the pressure gradient established in the porous catalyst pellet.

(2) Calculation of the nonisobaric effectiveness factor and comparison of it with the isobaric one for every flow and diffusion regime, from Knudsen to Poiseuille.

FUNDAMENTALS

The Equations of the Phenomenon

In order to reach our goal, the following working hypotheses will be assumed:

(a) The chemical reaction rate is given by:

$$r_A = k y_A^m P^m \tag{3}$$

(b) the catalyst pellet is spherical and isothermal

(c) the gaseous mixture is binary

(d) the system has reached the steady state.

Taking into account the previous restrictions, the behaviour of the system may be described by the following equations:

the diffusive flux of A,

$$N_{A1} = -\frac{D_{AB}D_{AA}^K}{(D_{AB} + D_{AA}^K)}\frac{1}{RT}\frac{dP_A}{dr} + \frac{y_A D_{AA}^K}{(D_{AB} + D_{AA}^K)}(N_{A1} + N_{B1}) \tag{4}$$

the diffusive flux of B,

$$N_{B1} = -\frac{D_{AB}D_{BB}^K}{(D_{AB} + D_{BB}^K)}\frac{1}{RT}\frac{dP_B}{dr} + \frac{y_B D_{BB}^K}{(D_{AB} + D_{BB}^K)}(N_{A1} + N_{B1}) \tag{5}$$

the viscous flux of A,

$$N_{A2} = -\frac{c_0 P_A}{\mu_m RT}\frac{dP}{dr} \tag{6}$$

the total flux of A,

$$N_A = N_{A1} + N_{A2} \tag{7}$$

the relationships between mole fractions and pressures, assuming ideal behavior,

$$P_A = y_A P \tag{8}$$

$$P_B = y_B P \tag{9}$$

$$y_A + y_B = 1 \tag{10}$$

the relationship between total fluxes of A and B,

$$N_B = -nN_A \tag{11}$$

the continuity equation for A,

$$-\frac{1}{r^2}\frac{d}{dr}(r^2 N_A) = k y_A^m P^m \tag{12}$$

Equations (4), (5) and (7) are based on the extended dusty gas model (*8, 9*). The symbols used in the previous equations indicate:

N: radial molar flux
y: mole fraction
P: pressure
R: gas constant
T: absolute temperature
r: radial coordinate in the catalyst pellet
D_{AB}: bulk effective diffusivity
D^K: Knudsen effective diffusivity
c_0: permeability of the porous medium
μ_m: gaseous mixture viscosity

The subscripts 1 and 2 indicate diffusive and viscous flux, respectively. The well-known relationship.

$$-\frac{N_{B1}}{N_{A1}} = (M_A/M_B)^{1/2} = n^{1/2}, \tag{13}$$

is contained in the previous equations (*9*).

Fluxes of A and B

By rearranging Eqs. (4)–(10), and letting

$\dfrac{D_{BB}^K}{D_{AA}^K} = (M_A/M_B)^{1/2} = n^{1/2}$, it results (9)

$$-N_A = \frac{D_{AB}^0 P}{\{1 + (n^{0.5} - 1)y_A\}P + (D_{AB}^0/D_{AA}^K)} \times \frac{1}{RT}\frac{dy_A}{dr} + \frac{(y_A)}{RT} \times \left[\frac{n^{0.5}D_{AA}^K P + D_{AB}^0}{\{1 + (n^{0.5} - 1)y_A\}P + (D_{AB}^0/D_{AA}^K)} + \frac{c_0 P}{\mu_m}\right]\frac{dP}{dr}, \tag{14}$$

where $D_{AB}^0 = D_{AB}P$ is a coefficient independent of pressure.

In deriving Eq. (14) it is not necessary to consider the slip flow separately (*9*). This is another difference with the development of Reference (*7*), where the slip flow is included as an independent contribution, a traditional result for flow in capillaries which is not valid for porous media.

It will be assumed that the gaseous mixture viscosity μ_{m} verifies Wilke's empiric equation (*10*),

$$\mu_{\mathrm{m}} = \frac{y_{\mathrm{A}}\mu_{\mathrm{A}}}{y_{\mathrm{A}} + (1 - y_{\mathrm{A}})\Phi_{\mathrm{AB}}} + \frac{(1 - y_{\mathrm{A}})\mu_{\mathrm{B}}}{(1 - y_{\mathrm{A}}) + y_{\mathrm{A}}\Phi_{\mathrm{BA}}}, \quad (15)$$

where

$$\Phi_{\mathrm{AB}} = (1/\sqrt{8})(1 + n)^{-1/2} \times \{1 + (\mu_{\mathrm{A}}/\mu_{\mathrm{B}})^{1/2}n^{-1/4}\}^2 \quad (16)$$

$$\Phi_{\mathrm{BA}} = (1/\sqrt{8})(1 + 1/n)^{-1/2} \times \{1 + (\mu_{\mathrm{B}}/\mu_{\mathrm{A}})^{1/2}n^{1/4}\}^2 \quad (17)$$

The $\mu_{\mathrm{A}}/\mu_{\mathrm{B}}$ relationship may be calculated as

$$\mu_{\mathrm{A}}/\mu_{\mathrm{B}} = (M_{\mathrm{A}}/M_{\mathrm{B}})^{1/2} = \sqrt{n} \quad (18)$$

From Eqs. (15–18),

$$\mu_{\mathrm{m}} = \{[1 + (4\{1 - y_{\mathrm{A}}\}/y_{\mathrm{A}})(8\{1 + n\})^{-0.5}]^{-1} + n^{-0.5}[(1 + [4y_{\mathrm{A}}/\{1 - y_{\mathrm{A}}\}]) \times (8\{1 + 1/n\})^{-0.5}]^{-1}\}\mu_{\mathrm{A}} \quad (19)$$

Equation (19) enables us to express μ_{m} in Eq. (14) as a function of μ_{A} and y_{A}. Equation (14) contains two dependent variables, P and y_{A}. Hence, we need a $P = P(r)$ relationship or a $P = P(y_{\mathrm{A}})$ function which may then be introduced in Eq. (14). This latter relationship may be obtained by the following procedure.

First, an analogous equation to Eq. (14) is written for the total flux of B in the porous medium,

$$-N_{\mathrm{B}} = \frac{n^{0.5}D_{\mathrm{AB}}{}^{0}P}{\{1 + (n^{0.5} - 1)y_{\mathrm{A}}\}P + (D_{\mathrm{AB}}{}^{0}/D_{\mathrm{AA}}{}^{\mathrm{K}})} \times \frac{1}{RT}\frac{\mathrm{d}y_{\mathrm{B}}}{\mathrm{d}r} + \frac{(1 - y_{\mathrm{A}})}{RT} \times \left[\frac{n^{0.5}(D_{\mathrm{AA}}{}^{\mathrm{K}}P + D_{\mathrm{AB}}{}^{0})}{\{1 + (n^{0.5} - 1)y_{\mathrm{A}}\}P + (D_{\mathrm{AB}}{}^{0}/D_{\mathrm{AA}}{}^{\mathrm{K}})} + \frac{c_0P}{\mu_{\mathrm{m}}}\right]\frac{\mathrm{d}P}{\mathrm{d}r} \quad (20)$$

By dividing Eq. (14) by Eq. (20), with the aid of Eqs. (10) and (11), and after some rearrangements, the following expression is obtained,

$$\frac{(n^{0.5} - n)\mathrm{d}y_{\mathrm{A}}}{1 + (n - 1)y_{\mathrm{A}}} = \left[\frac{n^{0.5}D_{\mathrm{AA}}{}^{\mathrm{K}}}{D_{\mathrm{AB}}{}^{0}} + \frac{c_0}{\mu_{\mathrm{m}}D_{\mathrm{AA}}{}^{\mathrm{K}}} + \frac{c_0P}{\mu_{\mathrm{m}}D_{\mathrm{AB}}{}^{0}} + \frac{c_0(n^{0.5} - 1)Py_{\mathrm{A}}}{\mu_{\mathrm{m}}D_{\mathrm{AB}}{}^{0}}\right]\mathrm{d}P + \left[\frac{n^{-0.5} + (1 - n^{-0.5})y_{\mathrm{A}}}{(1/n) + (1 - 1/n)y_{\mathrm{A}}}\right]\frac{\mathrm{d}P}{P} \quad (21)$$

So, by taking into account the pressure P may be related to the mole fraction y_{A} through Eq. (21), Eq. (14) may be written as,

$$-N_{\mathrm{A}} = f_1(P,y_{\mathrm{A}})(\mathrm{d}y_{\mathrm{A}}/\mathrm{d}r) + f_2(P,y_{\mathrm{A}})(\mathrm{d}P/\mathrm{d}y_{\mathrm{A}})(\mathrm{d}y_{\mathrm{A}}/\mathrm{d}r), \quad (22)$$

where:

$$f_1(P,y_{\mathrm{A}}) = \frac{D_{\mathrm{AB}}{}^{0}P}{\{1 + (n^{0.5} - 1)y_{\mathrm{A}}\}P + (D_{\mathrm{AB}}{}^{0}/D_{\mathrm{AA}}{}^{\mathrm{K}})} \times \frac{1}{RT} \quad (23)$$

$$f_2(P,y_{\mathrm{A}}) = \frac{y_{\mathrm{A}}}{RT} \times \left[\frac{n^{0.5}D_{\mathrm{AA}}{}^{\mathrm{K}}P + D_{\mathrm{AB}}{}^{0}}{\{1 + (n^{0.5} - 1)y_{\mathrm{A}}\}P + (D_{\mathrm{AB}}{}^{0}/D_{\mathrm{AA}}{}^{\mathrm{K}})} + \frac{c_0P}{\mu_{\mathrm{m}}}\right] \quad (24)$$

$$\frac{\mathrm{d}P}{\mathrm{d}y_{\mathrm{A}}} = \frac{(n^{0.5} - n)}{[1 + (n - 1)y_{\mathrm{A}}]\left[\frac{n^{0.5}D_{\mathrm{AA}}{}^{\mathrm{K}}}{D_{\mathrm{AB}}{}^{0}} + \frac{c_0}{\mu_{\mathrm{m}}D_{\mathrm{AA}}{}^{\mathrm{K}}}\left(1 + \frac{D_{\mathrm{AA}}{}^{\mathrm{K}}P}{D_{\mathrm{AB}}{}^{0}} + \frac{(n^{0.5} - 1)Py_{\mathrm{A}}D_{\mathrm{AA}}{}^{\mathrm{K}}}{D_{\mathrm{AB}}{}^{0}}\right) + \frac{1}{P}\left(\frac{n^{0.5} + (n - n^{0.5})y_{\mathrm{A}}}{1 + (n - 1)y_{\mathrm{A}}}\right)\right]} \quad (25)$$

Equation (25) can be easily obtained from Eq. (21). A convenient way of writing Eq. (22) is,

$$-N_A = f_3(P,y_A)(\mathrm{d}y_A/\mathrm{d}r), \tag{26}$$

where

$$f_3(P,y_A) = f_1(P,y_A) + f_2(P,y_A)(\mathrm{d}P/\mathrm{d}y_A)$$

The Flux of A with Simultaneous Chemical Reaction

So far, an expression for the total flux of A has been obtained. We may now rearrange the continuity equation for A, namely Eq. (12), which may be written as,

$$\frac{\mathrm{d}N_A}{\mathrm{d}r} + \frac{2}{r}N_A = -ky_AP \tag{27}$$

By differentiating Eq. (26) with respect to r,

$$-\frac{\mathrm{d}N_A}{\mathrm{d}r} = f_3(P,y_A)\frac{\mathrm{d}^2y_A}{\mathrm{d}r^2} + f_4(P,y_A)(\mathrm{d}y_A/\mathrm{d}r)^2, \tag{28}$$

where

$$f_4(P,y_A) = \frac{\partial f_3(P,y_A)}{\partial P}\frac{\mathrm{d}P}{\mathrm{d}y_A} + \frac{\partial f_3(P,y_A)}{\partial y_A} \tag{29}$$

By introducing Eqs. (26) and (28) in Eq. (27),

$$\frac{\mathrm{d}^2y_A}{\mathrm{d}r^2} + \frac{2}{r}\frac{\mathrm{d}y_A}{\mathrm{d}r} + \frac{f_4(P,y_A)}{f_3(P,y_A)}\left[\frac{\mathrm{d}y_A}{\mathrm{d}r}\right]^2 = \frac{ky_A{}^mP^m}{f_3(P,y_A)} \tag{30}$$

In order to integrate Eq. (30) it is convenient to write it in a dimensionless way,

$$\frac{\mathrm{d}^2y_A{}^*}{\mathrm{d}r^{*2}} + \frac{2}{r^*}\frac{\mathrm{d}y_A{}^*}{\mathrm{d}r^*} + g_1(P^*,y_A{}^*,H^*,D^*,y_{A0},n) \times \left(\frac{\mathrm{d}y_A{}^*}{\mathrm{d}r^*}\right)^2 = \frac{18h_0{}^2y_A{}^{*m}P^{*m}}{(m+1)g_2(P^*,y_A{}^*,H^*,D^*,y_{A0},n)}, \tag{31}$$

where

$$r^* = r/R_0$$

$$y_A{}^* = y_A/y_{A0}$$

$$P^* = P/P_0$$

$$H^* = c_0P_0{}^2/\mu_AD_{AB}{}^0$$

$$D^* = D_{AA}{}^KP_0/D_{AB}{}^0$$

$$g_1(P^*,y_A{}^*,H^*,D^*,y_{A0},n) = y_{A0}\frac{f_4(P^*,y_A{}^*,H^*,D^*,y_{A0},n)}{f_3(P^*,y_A{}^*,H^*,D^*,y_{A0},n)}$$

$$g_2(P^*,y_A{}^*,H^*,D^*,y_{A0},n) = f_3(P^*,y_A{}^*,H^*,D^*,y_{A0},n) \times (1 + 1/D^*)(RT/D_{AB}{}^0)$$

$$h_0 = \frac{R_0}{3}\left[\frac{(m+1)}{2}\frac{k(RT)P_{A0}{}^{(m-1)}}{D^R}\right]^{0.5}$$

$$\frac{1}{D^R} = \frac{P_0}{D_{AB}{}^0} + \frac{1}{D_{AA}{}^K}$$

The dimensionless groups H^* and D^* represent the ratio between the viscous flow coefficient and Knudsen effective diffusivity with respect to the bulk effective diffusivity, respectively. The parameter h_0 is the generalized Thiele modulus of the system. The subscript 0 indicates in every case the parameter or variable must be evaluated at the boundary of the catalyst pellet ($r = R_0$).

The g_1 and g_2 functions are developed in the Appendix.

The corresponding $P^* = P^*(y_A{}^*)$ may be obtained by solving Eq. (25) written in dimensionless form,

$$\frac{\mathrm{d}P^*}{\mathrm{d}y_A{}^*} = \frac{1}{B_1(y_A{}^*)\{n^{0.5}D^* + [H^*/B_2(y_A{}^*)][(1/D^*) + (B_4(y_A{}^*)P^*)] + (B_3(y_A{}^*)/P^*)\}}, \tag{32}$$

where the B_1 to B_4 functions are indicated in the Appendix.

Radial profiles of pressure and composition can be obtained by integrating Eqs. (31) and (32), with the following boundary conditions:

$$\begin{array}{ll} r^* = 0 & \mathrm{d}y_A{}^*/\mathrm{d}r^* = 0 \\ r^* = 1 & y_A{}^* = 1 \\ r^* = 1 & P^* = 1 \end{array} \tag{33}$$

On the other hand, the effectiveness factor of the catalyst pellet is defined as,

$$\eta_{\mathrm{I}} = -\frac{4\pi R_0^2 N_{\mathrm{A}}|_{r=R0}}{(4/3)\pi R_0^3 k y_{\mathrm{A}0}^m p_0^m} \tag{34}$$

By using Eq. (26) and the g_2 and h_0 definitions, Eq. (34) turns out to

$$\eta_{\mathrm{I}} = \frac{(m+1)}{6} \frac{(g_2 \mathrm{d}y_{\mathrm{A}}^*/\mathrm{d}r^*)|_{r^*=1}}{h_0^2} \tag{35}$$

Hence, the effectiveness factor η_{I} takes into account the influence of the radial composition and pressure profiles upon the chemical reaction rate.

By analyzing the radial composition profiles developed by nonequimolarity in chemical reaction, but considering that pressure remains constant through the catalyst pellet, another effectiveness factor, namely η_{II}, may be defined. Thus, by taking $\mathrm{d}P/\mathrm{d}r = 0$ in Eq. (14) and following the same steps leading to Eq. (31), it results:

$$\frac{\mathrm{d}^2 y_{\mathrm{A}}^*}{\mathrm{d}r^{*2}} + \frac{2}{r^*}\frac{\mathrm{d}y_{\mathrm{A}}^*}{\mathrm{d}r^*} + g_3(y_{\mathrm{A}}^*, D^*, y_{\mathrm{A}0}, n)\left(\frac{\mathrm{d}y_{\mathrm{A}}^*}{\mathrm{d}r^*}\right)^2 = \frac{18}{(m+1)} \frac{h_0^2 y_{\mathrm{A}}^{*m}}{g_4(y_{\mathrm{A}}^*, D^*, y_{\mathrm{A}0}, n)} \tag{36}$$

The g_3 and g_4 functions are developed in the Appendix. Hence, the effectiveness factor η_{II} is defined as,

$$\eta_{\mathrm{II}} = \frac{(m+1)}{6} \frac{g_4 \cdot \mathrm{d}y_{\mathrm{A}}^*/\mathrm{d}r^*|_{r^*=1}}{h_0^2} \tag{37}$$

Finally, by considering the radial composition profiles developed by an equimolar chemical reaction, the classical effectiveness factor, namely η_{III}, is easily obtained. Thus, letting $n = 1$ in Eq. (36) (then $g_3 = 0$, and $g_4 = 1$), the corresponding differential equation results,

$$\frac{\mathrm{d}^2 y_{\mathrm{A}}^*}{\mathrm{d}r^{*2}} + \frac{2}{r^*}\frac{\mathrm{d}y_{\mathrm{A}}^*}{\mathrm{d}r^*} = \frac{18 h_0^2}{(m+1)} y_{\mathrm{A}}^{*m} \tag{38}$$

So, the effectiveness factor η_{III} is given by,

$$\eta_{\mathrm{III}} = \frac{(m+1)}{6} \frac{(\mathrm{d}y_{\mathrm{A}}^*/\mathrm{d}r^*)|_{r^*=1}}{h_0^2} \tag{39}$$

The fact that a resultant effective diffusivity has been employed when defining the generalized Thiele modulus h_0, makes the equimolar effectiveness factor η_{III} independent of the diffusion regime (η_{III} does not depend on the D^* value).

The previous definitions may be summarized as follows: η_{I} is the nonisobaric, nonequimolar effectiveness factor, η_{II} is the nonequimolar but isobaric effectiveness factor, and η_{III} is the equimolar and, thus, isobaric effectiveness factor of the catalyst pellet.

INTEGRATION OF THE DIFFERENTIAL EQUATIONS

Differential Eqs. (31), (32), (36), and (38) were solved by applying the fourth order Runge-Kutta numerical method (*11*), and with the aid of an IBM/360 digital computer. When solving Eqs. (31), (36), (38), the variables change suggested by J. Wei, and analyzed in Reference (*12*), was performed. In this way, the solution could be obtained without using a trial an error method for checking the boundary conditions. In order to perform the solution of Eq. (31) the $P^* = P^*(y_{\mathrm{A}}^*)$ relationship obtained by solving Eq. (32) was introduced in the computation program. Besides, by combining both results, namely $P^* = P^*(y_{\mathrm{A}}^*)$ and $y_{\mathrm{A}}^* = y_{\mathrm{A}}^*(r^*)$, radial pressure profiles were obtained.

The computation program was verified as:

(a) an increase in the number of radial increments showed constancy of numerical values of the solutions

(b) the classical η_{III} vs h_0 relationship for first order reaction ($m = 1$) was obtained when solving Eq. (38).

RESULTS

The dimensionless parameters of the system were selected in the following range:

D^*: 0.01–100, corresponding to a change in the diffusion regime from Knudsen to bulk mechanisms

H^*: 0.01–100, corresponding to an increase in the permeability of the porous medium;

n: 0.1–10

$y_{\mathrm{A}0}$: 0.1–0.9

m: 1; 0.5

Results are illustrated in Figs. 1–9. Figure 1 shows radial composition and

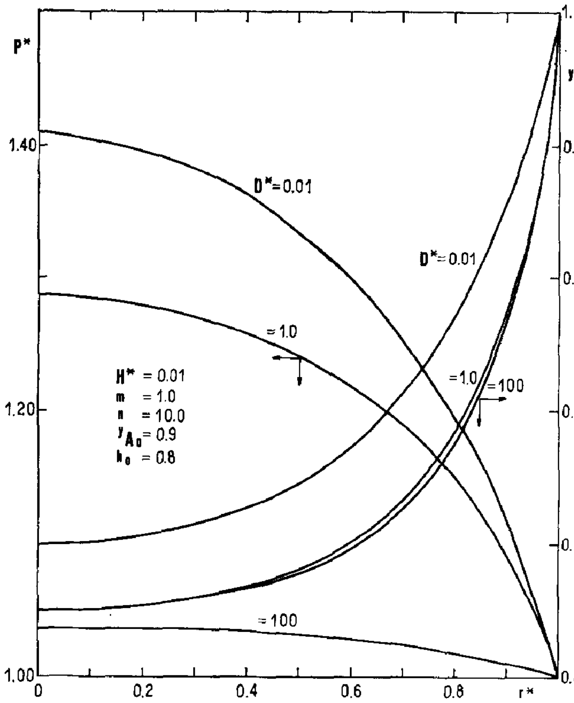

FIG. 1. Radial total pressure and mole fraction profiles in the catalyst pellet for $H^* = 0.01$.

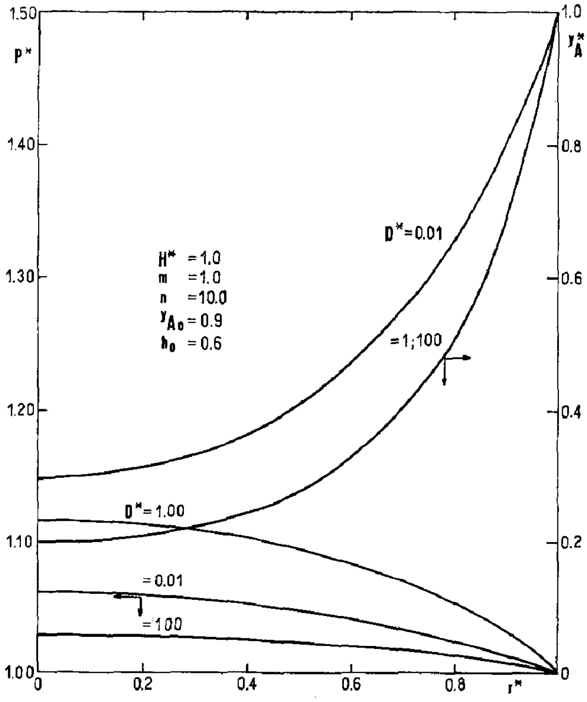

FIG. 2. Radial total pressure and mole fraction profiles in the catalyst pellet for $H^* = 1.0$.

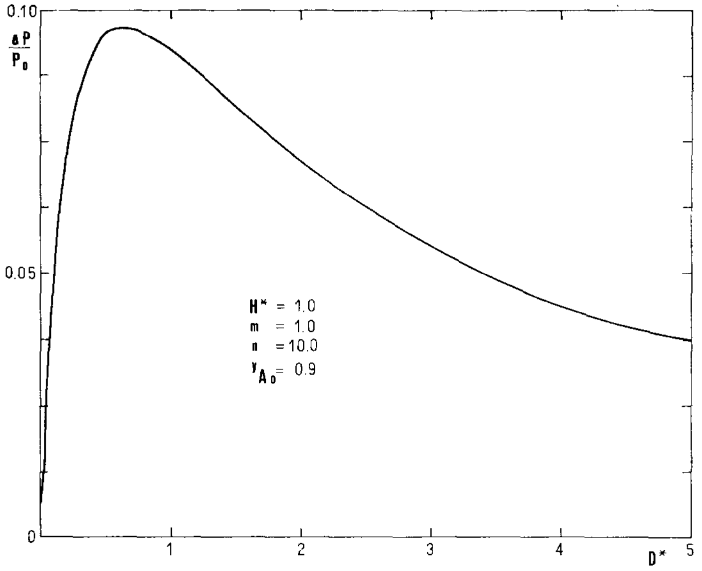

FIG. 3. Maximum dimensionless pressure difference in the catalyst pellet as a function of D^*.

pressure profiles for low values of the porous solid permeability ($H^* = 0.01$) and every diffusion regime. The pressure gradient reaches a significant figure for Knudsen and transition diffusion regimes, but is considerably depressed in the bulk diffusion one. Figure 2 shows the same radial profiles for greater values of the porous medium permeability ($H^* = 1.0$). Values of the radial pressure gradient are lower than those in the first case. When $H^* = 100$, the pressure gradient is considerably low though different than zero (this result is not plotted).

It is interesting to emphasize the inversion in the curves of $P^* = P^*(r^*)$ with respect to D^* showed in Fig. 2. This effect has been illustrated in Fig. 3 as a plot of $\Delta P/P_0$ vs D^*,ΔP being the pressure difference between the center and the boundary of the catalyst pellet. The resulting curve reaches the maximum at $D^* = 0.6$. For lower D^* values, ΔP is considerably depressed, thus leading to the inversion showed in Fig. 2.

Figures 4–6 show the effectiveness factor η_i (i = I, II, III) as a function of the Thiele modulus h_0, for every diffusion regime. It may be seen that the nonisobaric effectiveness factor, η_{I}, is considerably different from the isobaric one, η_{II}, for all diffusion regimes. η_{II} is in turn dif-

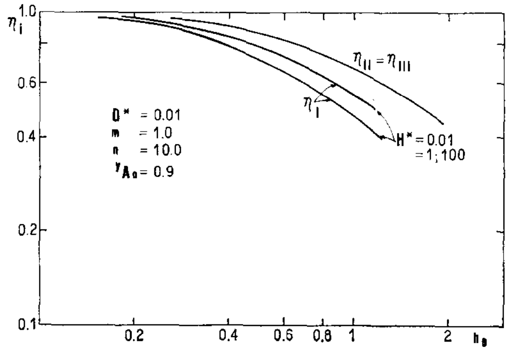

FIG. 4. Effectiveness factor vs Thiele modulus for Knudsen diffusion regime.

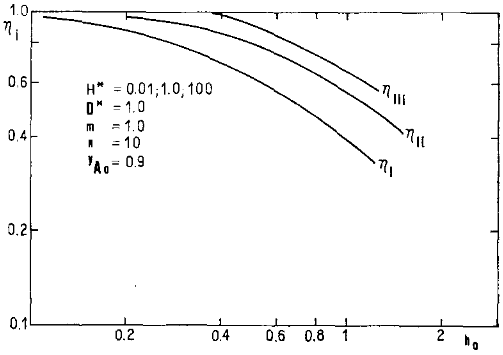

FIG. 5. Effectiveness factor vs Thiele modulus for transition diffusion regime.

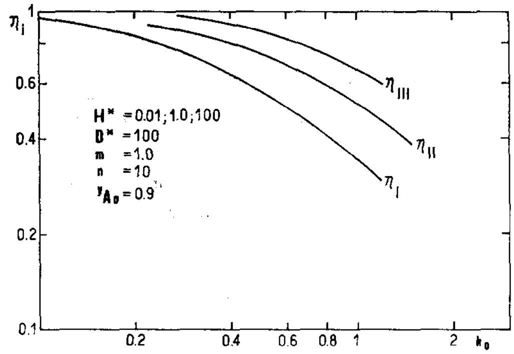

FIG. 6. Effectiveness factor vs Thiele modulus for bulk diffusion regime.

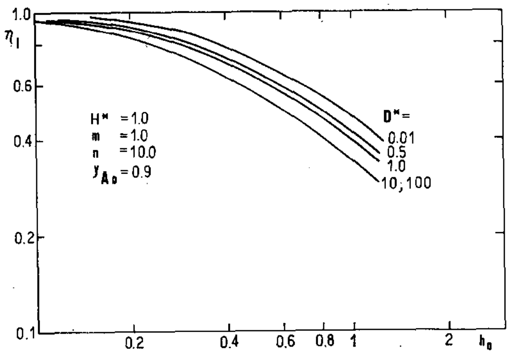

FIG. 8. Effect of D^* on the nonisobaric effectiveness factor.

ferent from η_{III} except in Knudsen diffusional regime. It is interesting to point out the low incidence of the H^* value upon the nonisobaric effectiveness factor in every diffusion regime.

Figure 7 indicates the effect of the change in the number of moles of the chemical reaction, n, upon the nonisobaric effectiveness factor. This factor is greater than the equimolar one (η_{III}) when $\eta < 1$, and lower when $n > 1$.

Figure 8 shows curves of η_I vs h_0 for different values of D^*. It is seen the higher the value of D^*, the lower the corresponding value of the nonisobaric effectiveness factor.

In Fig. 9, curves of η_I vs h_0 are plotted for various n and a different reaction order ($m = 0.5$).

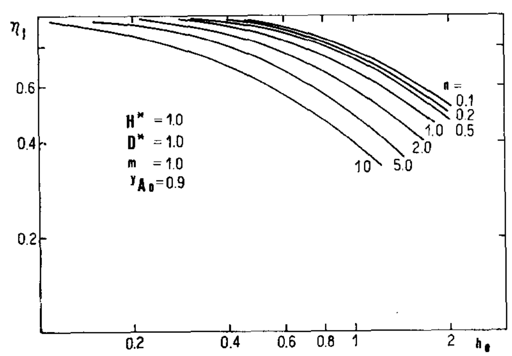

FIG. 7. Effect of the number of moles produced in the chemical reaction upon the nonisobaric effectiveness factor.

DISCUSSION OF RESULTS

Radial Pressure Profiles in the Catalyst Pellet

The radial pressure gradient is a function of the dimensionless parameters H^* and D^*. An increase in the first one, related to a higher permeability of the porous medium, diminishes the pressure gradient. However, as can be seen in Fig. 3, the variation of ΔP with D^* reaches a maximum. Mathematically, the existence of this maximum is easily justified by analyzing Eq. (32). The corresponding physical interpretation arises when Fig. 3 is regarded as a plot of ΔP vs P_0 (D^* being proportional to P_0, and H^* constancy requiring a continuous change either in the permeability or in the viscosity). At low working pressures (Knudsen diffusion regime) ΔP is proportional to P, while at greater working pressures (viscous flow

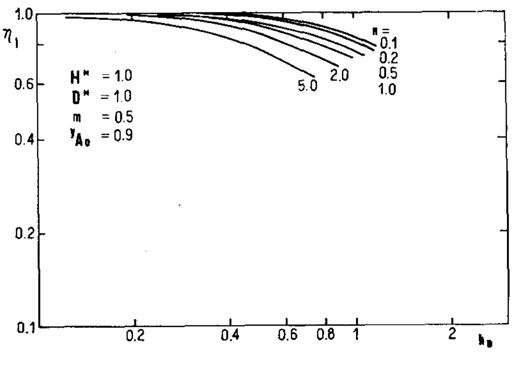

FIG. 9. Nonisobaric effectiveness factor for reaction order $m = 0.5$.

regime), ΔP is proportional to P^{-1}. The maximum arises when both effects are combined. It is convenient to point out that the existence of the maximum in the ΔP vs P function was theoretically predicted (*8*) for a binary gaseous mixture in a closed system without chemical reaction (Kramers–Kistemaker effect).

Nonisobaric Effectiveness Factor

Results of Figs. 4–7 show that the nonisobaric effectiveness factor is considerably different from the isobaric one, even for values of $n = 0.5$ and 2, and for every mass transport regime. This indicates that even in the cases in which pressure gradient is almost negligible (high H^* values) the flow produced by this gradient is very significant. That is to say, the pressure gradient is almost negligible just because the flux coefficient H^* is high.

In fact, the system under analysis is a semi-closed one. Then, the pressure gradient can not be established at will by us but it adjusts automatically in accordance to the prevailing mass transport regime. In this situation, a low value of the pressure gradient does not involve that the resultant flux is negligible.

As the nonequimolar flow is characteristic of the bulk diffusion regime, it must be verified that $\eta_{\text{II}} = \eta_{\text{III}}$ in Knudsen diffusion pattern. This is just the result plotted in Fig. 4, which gives an extra verification of the consistency of the numerical calculations. However, even in Knudsen diffusion regime, the non-isobaric effectiveness factor is considerably different from the isobaric one.

In order to show the low incidence of the H^* value upon the non-isobaric effectiveness factor, let us rewrite Eq. (22) in the following way:

$$\frac{N_{\text{A}}}{\mathrm{d}y_{\text{A}}/\mathrm{d}r} = f_1(P,y_{\text{A}}) + f'_2(P,y_{\text{A}})(\mathrm{d}P/\mathrm{d}y_{\text{A}}) + f''_2(P,y_{\text{A}})(\mathrm{d}P/\mathrm{d}y_{\text{A}}), \quad (40)$$

where:

$$f'_2(P,y_{\text{A}}) = \frac{y_{\text{A}}}{RT}\left[\frac{n^{0.5}D_{\text{AA}}{}^{\text{K}}P + D_{\text{AB}}{}^0}{\{1 + (n^{0.5} - 1)y_{\text{A}}\}P + (D_{\text{AB}}{}^0/D_{\text{AA}}{}^{\text{K}})}\right] \quad (41)$$

$$f''_2(P,y_{\text{A}}) = \frac{y_{\text{A}}}{RT}\left(\frac{c_0P}{\mu_{\text{m}}}\right) \quad (42)$$

The three terms of the right-hand side of Eq. (40) represent fluxes of A per unit of its mole fraction gradient generated, respectively, by mole fraction gradient (diffusive flux), total pressure gradient (diffusive flux) and total pressure gradient (viscous flux).

The terms may be rearranged as:

$$F_{\text{D}} = f'_2(P,y_{\text{A}})\frac{\mathrm{d}P}{\mathrm{d}y_{\text{A}}}/f_1(P,y_{\text{A}}) \quad (43)$$

$$F_{\text{V}} = f''_2(P,y_{\text{A}})\frac{\mathrm{d}P}{\mathrm{d}y_{\text{A}}}/f_1(P,y_{\text{A}}), \quad (44)$$

where F_{D} represents the ratio between the diffusive flux generated by total pressure gradients with respect to the diffusive flux generated by mole fraction gradients; and F_{V} corresponds to the ratio between viscous flux and diffusive flux produced by mole fraction gradients.

Figure 10 shows curves of F_{D} and F_{V} as a function of H^*. As may be seen from the figure, the addition of both fluxes does not depend on the H^* value, which is the cause of the low incidence of the H^* value upon the nonisobaric effectiveness factor. Besides, Fig. 10 shows that for high H^* values, and consequently low values of the pressure gradient, the resulting viscous flow is very significant, and accounts for the important deviations between η_{I} and η_{II}.

The variation of the nonisobaric effectiveness factor with D^*, plotted in Fig. 8, would lead to the rather misleading conclusion that the greater the tendency to bulk diffusion regime, the lower the effectiveness factor. In doing this statement one must not forget that the Thiele modulus has been defined in terms of a resultant diffusivity which, in fact, is a function of D^*. If the Thiele modulus had been defined with the bulk diffusivity, the curves would have shown just an opposite variation with D^*.

On the other hand, an increase in the mole fraction of A at the boundary of the catalyst pellet diminishes the nonisobaric effectiveness factor when $n > 1$. However, the decrease is negligible for $1 < n < 5$,

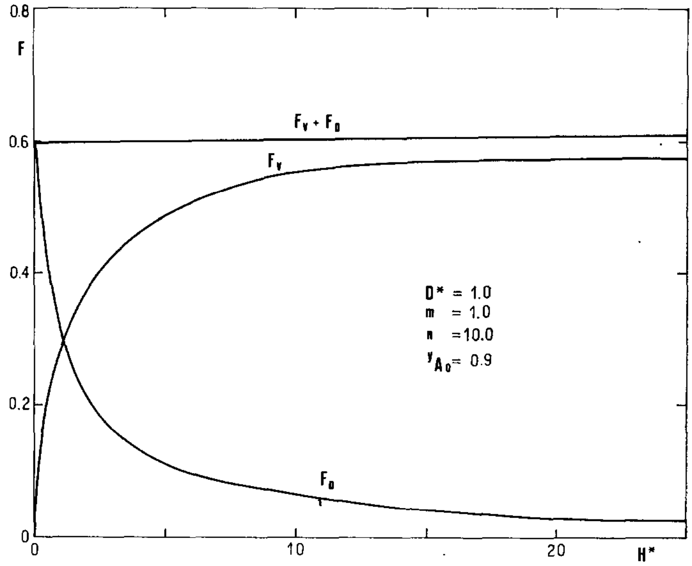

FIG. 10. Fluxes originated by total pressure gradients, as a function of H^*.

and is not important for higher values of n. (These results are not plotted herewith.)

CONCLUSIONS

Results obtained by numerical integration of the proper differential equations show that the nonisobaric effectiveness factor is considerably different from the isobaric one, even for small changes in the number of moles during the chemical reaction, and for every flow regime. This in turn demonstrates that, in semi-closed systems, small pressure gradients can not be considered negligible because the resulting flow (the product of a flux coefficient times a gradient) is quite significant.

Besides, it has been shown that the pressure difference between the center and the boundary of the catalyst pellet reaches a maximum value for a given working pressure.

APPENDIX

The g_i and B_i (i = 1-4) functions used in the present study, can be written as follows:

$$g_1 = A_1(A_2 + A_3 + A_4 + A_5 - A_6) \qquad (45)$$

$$g_2 = (1 + 1/D^*)\left(A_7 + \frac{y_A^* A_8}{A_9 A_{10}}\right) \qquad (46)$$

$$g_3 = \frac{(1 - n^{0.5})y_{A0}}{A_{11}} \qquad (47)$$

$$g_4 = \frac{(1 + 1/D^*)}{A_{11}} \qquad (48)$$

$$B_1 = A_9 \qquad (49)$$

$$B_2 = A_{17} + A_{18} \qquad (50)$$

$$B_3 = \left[\frac{n^{0.5} + (n - n^{0.5})y_{A0}y_A^*}{1 + (n - 1)y_{A0}y_A^*}\right] \qquad (52)$$

$$B_4 = \{1 + y_{A0}(n^{0.5} - 1)y_A^*\}, \qquad (53)$$

where:

$$A_1 = 1/\left(A_7 + \frac{y_A^* A_8}{A_9 A_{10}}\right)$$

$$A_2 = \frac{(1/\{D^*P^{*2}\})A_7^2}{A_9 A_{10}}$$

$$A_3 = \frac{y_A^*(A_{12} - A_{13})}{A_9^2 A_{10}^3}$$

$$A_4 = (1 - n^{0.5})y_{A0}A_7^2$$

$$A_5 = \frac{A_8 + y_A^*\{(A_4(1 + n^{0.5}D^*P^*)/P^*) - A_{14}A_{15}\}}{A_9 A_{10}}$$

$$A_6 = y_A^* A_8 A_{16}/(A_9 A_{10})^2$$

$$A_7 = 1/\{1 + (n^{0.5} - 1)y_{A0}y_A^* + (1/D^*P^*)\}$$

$$A_8 = (1 + n^{0.5}D^*P^*)A_7/P^* + (H^*P^*)/(A_{17} + A_{18})$$

$$A_9 = \frac{1/y_{A0} + (n-1)y_A{}^*}{(n^{0.5} - n)}$$

$$A_{10} = n^{0.5}D^* + \{H^*(1/D^* + P^* \times \{1 + y_{A0}(n^{0.5} - 1)y_A{}^*\})/(A_{17} + A_{18})\}$$

$$A_{11} = \{1 + (n^{0.5} - 1)y_{A0}y_A{}^* + 1/D^*\}$$

$$A_{12} = A_{10} \times \left(\frac{\{n^{0.5} - (1 + \{n^{0.5} - 1\}y_{A0})y_A{}^*\}A_7{}^2}{P^{*2}}\right) + \frac{H^*}{A_{17} + A_{18}}$$

$$A_{13} = \{(H^*\{1 + (n^{0.5} - 1)y_{A0}y_A{}^*\})/(A_{17} + A_{18})\}A_8$$

$$A_{14} = \left\{\frac{A_{17}}{y_A{}^*} - \frac{[1 - 4\{8(1+n)\}^{-0.5}]A_{17}{}^2}{y_A{}^*} - \frac{A_{18}}{(1/y_{A0} - y_A{}^*)} + \frac{[-1 + 4\{8(1 + 1/n)\}^{-0.5}]A_{18}{}^2}{(1/y_{A0} - y_A{}^*)n^{-0.5}}\right\}$$

$$A_{15} = (H^*P^*)/(A_{17} + A_{18})^2$$

$$A_{16} = \frac{(n-1)}{(n^{0.5} - n)}A_{10} + \frac{A_9}{(A_{17} + A_{18})^2}(A_{19} - A_{20}A_{14})$$

$$A_{17} = y_A{}^*/[y_A{}^* + (1/y_{A0} - y_A{}^*) \times 4\{8(1+n)\}^{-0.5}]$$

$$A_{18} = \frac{(1/y_{A0} - y_A{}^*)n^{-0.5}}{(1/y_{A0} - y_A{}^*) + y_A{}^*4\{8(1 + 1/n)\}^{-0.5}}$$

$$A_{19} = (A_{17} + A_{18})\{H^*P^*(n^{0.5} - 1)y_{A0}\}$$

$$A_{20} = H^*\{1/D^* + P^*(1 + y_{A0}\{n^{0.5} - 1\}y_A{}^*)\}$$

References

1. Weekman, V. W., Jr., and Gorring, R. L., *J. Catal.* **4**, 260 (1965).
2. Kan Lih, and Lih, Marshall M., *AIChEJ.* **17**(5), 1234 (1971).
3. Evans, R. B., III, Watson, G. M., and Mason, E. A., *J. Chem. Phys.* **35**, 2076 (1961).
4. Evans, R. B., III, Watson, G. M., and Mason, E. A., *J. Chem. Phys.* **36**, 1894 (1962).
5. Mason, E. A., Evans, R. B., III, and Watson, G. M., *J. Chem. Phys.* **38**, 1808 (1963).
6. Otani, S., Wakao, N., and Smith, J. M., *AIChEJ.* **10**, 130 (1964).
7. Otani, S., Wakao, N., and Smith, J. M., *AIChEJ.* **11**, 446 (1965).
8. Mason, E. A., Malinauskas, A. P., and Evans, R. B., III, *J. Chem. Phys.* **46**, 3199 (1967).
9. Gunn, R. D., and King, C. Judson, *AIChEJ.* **15**, 507 (1969).
10. Bird, R. B., Stewart, W. E., and Lightfoot, E. N., "Transport Phenomena," John Wiley & Sons, New York, 1960.
11. Mickley, Harold, S., Sherwood, T. K., and Reed, C. E., "Applied Mathematics in Chemical Engineering," McGraw-Hill Book Co., Inc., Tokyo, 1957.
12. Weisz, P. B., and Hicks, J. S., *Chem. Eng. Sci.* **17**, 265 (1962).